

Hydrodynamical instability of spatially extended bistable chemical systems

A. De Wit^{a,*}, P. De Kepper^b, K. Benyaich^a, G. Dewel^a, P. Borckmans^a

^a*Service de Chimie Physique and Centre for Nonlinear Phenomena and Complex Systems, CP 231, Université Libre de Bruxelles, Brussels 1050, Belgium*

^b*Centre de Recherche Paul Pascal, CNRS, Université Bordeaux I, Avenue A. Schweitzer, 33600 Pessac, France*

Received 17 July 2002; received in revised form 25 November 2002; accepted 27 November 2002

Abstract

Hydrodynamical density fingering of chemical fronts separating two miscible, stable steady states of different chemical composition, and hence density, can lead to complex spatio-temporal dynamics. The most striking feature of such dynamics is the disconnection of droplets of one stable steady state from fingers invading the other stable steady state. Such disconnected droplets do not exist in pure density fingering and are thus the result of the bistable kinetics. We study such dynamics by direct numerical simulations of Darcy's law for flow in Hele–Shaw cells coupled to the kinetic equation for the concentration of a chemically reacting solute controlling the density of the miscible solutions. The concentration of this solute obeys a simple cubic model leading to bistability. Experimental realization of such dynamics in spatially extended Hele–Shaw cells calls for the use of the concept of spatial bistability which implies construction of new continuously fed open reactors.

© 2003 Elsevier Ltd. All rights reserved.

Keywords: Density fingering; Chemical composition; Spatio-temporal dynamics

1. Introduction

Chemical reactions can interact with hydrodynamical fingering instabilities and thereby affect the stability properties as well as the nonlinear spatio-temporal dynamics of the system. Recently, the coupling between miscible viscous fingering and bistable chemical reactions has been studied in chemical autocatalytic systems providing traveling fronts between miscible solutions of different viscosities (De Wit & Homsy, 1999a, b). It was shown that the bistable kinetics leads to detachment of droplets of one chemical state from fingers of the other state. Such a shedding of droplets was clearly linked to the fact that the two stable steady states of different viscosity are both attractors of the chemical kinetics. Unfortunately, experimental evidence of such new spatio-temporal dynamics has not been provided yet. The viscosity of a fluid usually depends on the concentration of solutes but the typical nonlinear reactions that provide traveling fronts have mostly been studied in aqueous solutions for which the viscosity is basically that of water in both the reactant and product solutions. However, the association

of nonlinear pH-driven reaction with appropriate charged soluble polymer could lead to considerable changes in the viscosity of the solution as a function of the pH of the solution but this remains to be explored.

Experiments on miscible viscous fingering in reactive systems have addressed the effect of the variation of reactant concentrations and of the finger pattern on the spatial distribution of chemical species showing that the flow can drastically influence the reaction (Nagatsu & Ueda, 2001). However, in these systems, the chemical reaction does not feed back on the hydrodynamical motion as the viscosity of the two solutions at hand is not influenced by the reactions. The only striking evidence of viscosity changes across a moving front due to reactions occurs in polymerization fronts where the monomer and the polymer solutions can exhibit quite strong differences in viscosity (Pojman, Gunn, Patterson, Owens, & Simmons, 1998; Epstein & Pojman, 1998). Nevertheless, in such miscible polymeric systems, no evidence of bistability exists as the transition from the monomer solution to the more viscous polymer is usually irreversible.

In this article, we show by numerical simulations that the coupling between miscible *density fingering* and bistable

* Corresponding author.

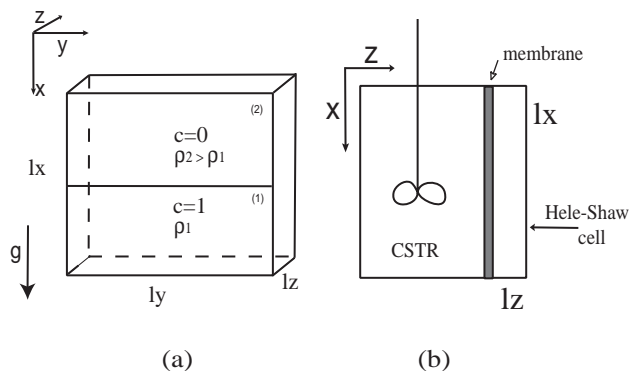


Fig. 1. Sketch of the open Hele–Shaw reactor. (a) front view showing the cell in the (x, y) plane containing two solutions of different composition and density; (b) lateral view of the (x, z) plane. Feeding of the Hele–Shaw cell is made by replacing one plate of the cell by a membrane in contact with a CSTR. Feeding is achieved along the (xy) plane at $z = 0$ while visualization is made along the opposite plane at $z = l_z$.

kinetics can lead to hydrodynamical instability of reaction–diffusion fronts and droplet formation as well. On the basis of the concept of spatial bistability, we discuss the possible experimental realization of such dynamics by implementing bistable kinetics in an open spatially extended reactor of Hele–Shaw geometry (two glass plates separated by a gap of thin width—see Fig. 1).

Chemical autocatalytic reactions such as for instance the iodate–arsenious acid (IAA) or chlorite–tetrathionate (CT) reactions are known to produce traveling fronts in aqueous solutions. These reactions exhibit the so-called “clock dynamics” in a batch reactor. For given initial concentrations, the reaction undergoes a sudden single switch towards thermodynamic equilibrium after an induction period. When such reactions are carried out in a continuously stirred tank reactor (CSTR) which is open to mass fluxes, they may feature bistability between steady states depending on the residence time in the reactor or the input concentration which both characterize the mass flow.

Such autocatalytic reactions are also known to provide density differences between reactants and products. These density changes across the front can drive buoyantly unstable situations as soon as the heavier solution lies on top of the lighter one in the gravity field. Fingering of the front then occurs. Experimental evidences (Nagypal, Bazsa, & Epstein, 1986; Pojman, Epstein, McManus, & Showalter, 1991; Chinake & Simoyi, 1994; Masere, Vasquez, Edwards, Wilder, & Showalter, 1994; Carey, Morris, & Kolodner, 1996; Böckmann & Müller, 2000; Horváth, Bánsági, & Tóth, 2002) and theoretical studies (Edwards, Wilder, & Showalter, 1991; Vasquez, Wilder, & Edwards, 1993; Huang & Edwards, 1996; McCaughey, Pojman, Simmons, & Volpert, 1998; Garbey, Taïk, & Volpert, 1998; De Wit, 2001; Martin, Rakotomalala, Salin, & Böckmann, 2002; Yang, D’Onofrio, Kalliadasis, & De Wit, 2002) on density-driven instabilities of chemical fronts have shown that the coupling between buoyancy-driven flows and the

chemical reactions can strongly affect the stability properties as well as the nonlinear dynamics of the fingering instability. Contrary to the viscous fingering set-up, where a fluid of given chemical composition (and thus viscosity) pushes away another more viscous fluid of different composition, the above-mentioned density fingering experiments are carried out in closed reactors. All these studies have focused on traveling fronts where the equilibrium state is invading an initial state that will undergo a spontaneous transition to equilibrium after a more or less long induction period. Here we want to consider the situation of a nonmoving front between two stable steady states of different densities. Therefore, one must somehow open the reactor to mass fluxes to create bistability. Bistability in spatially extended systems has been addressed for instance in studies of diffusive instabilities in numerous physico-chemical systems such as nonlinear optics, semiconductors, gas discharges, etc. (Firth, Scroggie, & McDonald, 1992; Ackemann, Logvin, Heuer, & Lange, 1995; Breazeal, Flynn, & Gwinn, 1995; Dewel, Métenens, Hilali, Borckmans, & Price, 1995; Métenens, Dewel, Borckmans, & Engelhardt, 1997; Bachir, Métenens, Borckmans, & Dewel, 2001). Considering the specific case of chemistry, the situation remains to be fully clarified as, contrary to the other systems, bistability is not a property of the intrinsic chemical kinetics but of the competition between this kinetics and the mass flow (Borckmans et al., 2002).

To account for this coupling between chemical reactions with inflow and outflow of the chemical species in the reactor, the so-called continuous-flow unstirred reactor (CFUR) approximation (Vastano, Pearson, Horsthemke, & Swinney, 1987; Pearson, 1993) has often been used and has been able to describe some of the reaction–diffusion structures and behaviors of the ferrocyanide–iodate–sulfite (FIS) reaction in thin spatial reactors (Lee, McCormick, Pearson, & Swinney, 1994; Lee & Swinney, 1995). In this approximation, the reactor is analogous to a two-dimensional reaction–diffusion system where each point of the system is directly fed by fresh reactants and releases all the species involved in the kinetic mechanism. The system is thus described by a 2D continuum of CSTRs coupled by diffusion and its dynamics obeys an equation of the type

$$\frac{\partial \mathbf{c}(\mathbf{r}, t)}{\partial t} = D \nabla^2 \mathbf{c}(\mathbf{r}, t) + \mathbf{f}(\mathbf{c}, b) + \frac{(\mathbf{c}_0 - \mathbf{c}(\mathbf{r}, t))}{\tau}, \quad (1)$$

where $\mathbf{c}(\mathbf{r}, t)$ stands for the concentration of the various chemical species in the reactor. \mathbf{c}_0 is the input concentration in the feeding of the CSTRs, D is the molecular diffusion coefficient while τ is the residence time of the chemical species in the CSTRs. For the clock reactions considered here and particularly for the IAA reaction, the presence of the two last terms in Eq. (1) may give rise to a cubic function of the concentrations thereby leading to bistability of homogeneous steady states (HSS). As an example, for the IAA reaction in a CSTR, kinetic studies show that in presence of excess of arsenous acid, the system is well described by the

following equation:

$$\frac{dc}{dt} = -qc(c - S_0)(c + \beta) + \frac{(c_0 - c)}{\tau}, \quad (2)$$

where $c = [I^-]$, $S_0 = [IO_3^-]_0 + [I^-]_0$ is the sum of the input iodate and iodide concentrations, $\beta = k_a/k_b$ where k_a and k_b are kinetic constants while $q = k_b[H^+]^2$. The kinetics in batch reactors (i.e. in absence of any flow term) admits one stable steady state $c = S_0$, one unstable steady state $c = 0$ and one solution $c = -\beta$ which is outside reaction space as the concentrations must always remain positive. Reordering the polynomial by taking the flow terms into account leads to a new cubic form $-q(c - A)(c - B)(c - D)$, which, for given flow rate $k_0 = 1/\tau$, can admit three real positive roots ($0 < A < B < D$). Defining $c' = c - A$, $c_1 = B - A$ and $c_2 = D - A$, the monostable kinetics operating in each CSTR with constant inflow and outflow such as in Eq. (2) is seen to be equivalent to the following bistable kinetics (after dropping the primes):

$$\frac{dc}{dt} = -qc(c - c_1)(c - c_2), \quad (3)$$

where the system now admits two stable HSS $c = 0, c_1$ and one unstable steady state $c = c_2$ with $0 < c_2 < c_1$ and where c_1 and c_2 are functions of S_0, β, q, τ and c_0 .

In Section 2, we make use of the CFUR approximation to study the nonlinear interplay between bistable chemical fronts and density-driven fingering in Hele–Shaw cells. We show that such fingering in an open Hele–Shaw cell may lead to the formation of droplets. We then discuss the characteristics of the fingering pattern and the influence of the bistable kinetics on it in Section 3. The importance of the concept of spatial bistability in the experimental realization of the pattern is addressed in Section 4, where we also discuss the implication of the notions of spatial bistability that go beyond the CFUR approximation.

2. Model system

Our model system is a Hele–Shaw cell of length l_x , width l_y and gap width l_z with $l_z \ll l_x, l_y$. The gravity field \underline{g} is oriented along x (see Fig. 1).

The flow inside the cell is modeled using the two-dimensional Darcy's law, a good approximation for small gap widths (Homsy, 1987). It is assumed that the density ρ of the fluid depends on the concentration c of a given reactive solute and that the initial configuration is a nonmoving front between two stable miscible solutions of differing chemical composition and hence of different density. This density difference is assumed to be small enough so that the Boussinesq assumption holds. The system then obeys the following set of equations:

$$\underline{\nabla} \cdot \underline{u} = 0, \quad (4)$$

$$\underline{\nabla} p = -\frac{\mu}{\kappa} \underline{u} + \rho(c) \underline{g}, \quad (5)$$

$$\rho(c) = \rho_1 + (\rho_2 - \rho_1) \left(1 - \frac{c}{c_1}\right), \quad (6)$$

$$\frac{\partial c}{\partial t} + \underline{u} \cdot \underline{\nabla} c = D \nabla^2 c - qc(c - c_1)(c - c_2), \quad (7)$$

where the viscosity μ and the molecular diffusion coefficient D are considered constant in space and time and p denotes the pressure. The permeability κ is equal to $l_z^2/12$ for thin Hele–Shaw cells. The kinetic scheme of Eq. (7) results from the CFUR approximation and is taken as a model for a bistable situation. The density depends linearly on the concentration with $\rho_2 = \rho(c = 0) > \rho_1 = \rho(c = c_1)$.

To nondimensionalize the equations, we define the characteristic hydrodynamical speed as $U = \Delta \rho g \kappa / \nu$ with $\Delta \rho = (\rho_2 - \rho_1) / \rho_1$ and $\nu = \mu / \rho_1$, the kinematic viscosity. We next choose $L = D/U$ and $\tau_h = D/U^2$ as respective characteristic length and time scales. The pressure, viscosity, density and concentrations are scaled by $\mu D / \kappa$, μ , ρ_1 and c_1 . In addition, we define a hydrostatic pressure gradient as $\underline{\nabla} p'' = \underline{\nabla} p' - \rho_1' \underline{i}_x$. Dropping all the primes, the evolution equations for the dimensionless variables become

$$\underline{\nabla} \cdot \underline{u} = 0, \quad (8)$$

$$\underline{\nabla} p = -\underline{u} + (1 - c) \underline{i}_x, \quad (9)$$

$$\frac{\partial c}{\partial t} + \underline{u} \cdot \underline{\nabla} c = \nabla^2 c - Da c(c - 1)(c - d) \quad (10)$$

with $d = c_2/c_1$ and $Da = Dqc_1^2/U^2$. Da is in fact the ratio τ_h/τ_c between the characteristic hydrodynamical time scale $\tau_h = D/U^2$ and the chemical time scale $\tau_c = 1/qc_1^2$, i.e. Da is the Damköhler number of the problem. The higher the Da , the faster the chemical time scale and hence the stronger the chemical effects with respect to the hydrodynamical effects. The dimensionless kinetics now admits two stable ($c = 0$ and 1) and one unstable $c = d$ ($0 < d < 1$) states where d is also the limit between the basins of attraction of $c = 0$ and 1 . The nondimensionalized width l_y/L takes the form of a Péclet number $Pe = l_y U/D$ and the aspect ratio of the system is $A = l_x/l_y$. Taking the curl of Eq. (9) and introducing the stream function ψ such that $u = \partial\psi/\partial y$ and $v = -\partial\psi/\partial x$, we obtain the final equations

$$\nabla^2 \psi = -c_y, \quad (11)$$

$$\frac{\partial c}{\partial t} + c_x \psi_y - c_y \psi_x = \nabla^2 c - Da c(c - 1)(c - d), \quad (12)$$

where the subscripts denote partial derivatives. In the absence of any flow ($\psi = 0$), Eq. (12) admits a propagating front solution between the two stable steady states (Hanna, Saul, & Showalter, 1982; Saul & Showalter, 1985):

$$\begin{aligned} c(x, t) &= \frac{1}{2} \left[1 + \tanh \left(-\sqrt{\frac{Da}{8}} (x - vt) \right) \right] \\ &= \frac{1}{1 + e^{-\sqrt{(Da/2)(x-vt)}}}, \end{aligned} \quad (13)$$

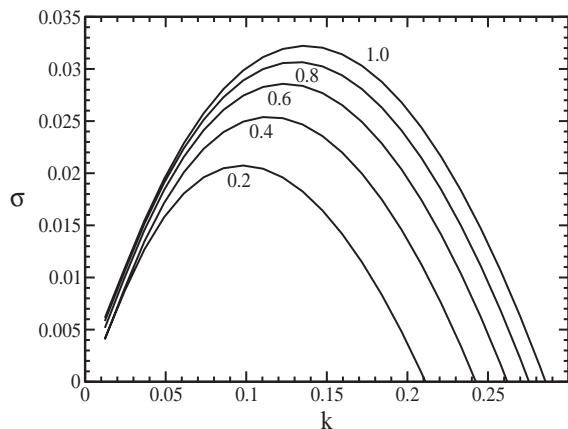


Fig. 2. Dispersion curves featuring the growth rate σ of the various modes as a function of their wavenumber k for increasing values of Da .

traveling with a velocity

$$v = \sqrt{\frac{Da}{2}}(1 - 2d). \quad (14)$$

Note that the width W of the chemical front, arbitrarily defined as the distance between $c=0.01$ and 0.99 , can readily be found from Eq. (13) to be equal to

$$W = \sqrt{\frac{8}{Da}} \ln(99). \quad (15)$$

Expressions (14) and (15) thus show that increasing Da leads to sharper waves traveling with a higher speed. In the following, we choose the peculiar value $d = 0.5$ such that the front between the two stable steady states $c = 0$ and 1 has zero velocity.

We have performed a linear stability analysis (LSA) of the planar traveling front (13) with regard to transverse (along y) disturbances along the lines described in De Wit (2001). Such an LSA allows to obtain dispersion curves featuring the growth rate σ of the disturbances as a function of their wavenumber k . Fig. 2 shows that there is a band of unstable modes ranging from $k = 0$ up to a critical value. Increasing the Damköhler number destabilizes the system which is then characterized by larger growth rates and higher most unstable wavenumber. Quick and sharp fronts between bistable states (high Da) will thus be more sensitive to fingering than slow and loose ones, a conclusion which is similar to that obtained for fronts of one stable state invading another unstable steady state (monostable case) as studied in De Wit (2001).

3. Droplet formation

Using pseudo-spectral methods (Tan & Homsy, 1988), we integrate model (11)–(12) taking as initial conditions $\psi = 0$ everywhere which corresponds to solutions convectively at rest. Periodic boundary conditions are used in both longitudinal and transverse directions. For the concentration,

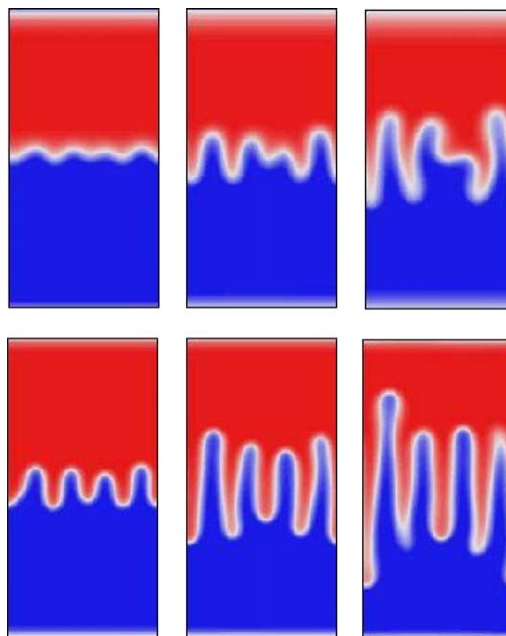


Fig. 3. Density fingering in a system of size $Pe = 512$, $A = 2$ shown from left to right at successive times $t = 1000$, 1500 and 2000 . The red and blue colors correspond to $c = 0$ and 1 , respectively. Upper line: pure density fingering in absence of chemical reactions ($Da = 0$). Lower line: density fingering in presence of chemical reactions for small Damköhler number ($Da = 0.01$, $d = 0.5$). The chemical reactions enhance the instability leading to a larger mixing length and an earlier appearance of fingers.

we start from a step function between $c = 0$ and 1 located at the center of the system and the reverse step function at the bottom with white noise of 0.1% in amplitude added at the fronts. The upper front corresponds to the heavier $c = 0$ state placed on top of the lighter $c = 1$ solution which, in the gravity field, corresponds to a buoyantly unstable situation leading to density fingering. The reverse front at the bottom is on the contrary stable and features simple diffusive mixing between the two miscible solutions when $Da = 0$ and a constant width given by Eq. (15) when $Da \neq 0$. If $Da = 0$, there is no chemical reaction and the model features pure density fingering as shown on the upper line of Fig. 3. Diffusion leads to the mixing of the two solutions in the course of time and a dilution of the mixing zone. If $Da \neq 0$, we analyze the effect of bistable chemical reactions on density fingering. Even for very small Da (see Fig. 3), the effect of the chemical reactions can clearly be seen as leading to higher growth rates (the fingers appear more quickly) and more elongated fingers. This tendency increases when Da is larger (compare Figs. 3 and 4), i.e. the wavelength of the fingers becomes smaller (larger wavenumber) and appear faster. This is coherent with the predictions of the linear stability analysis shown in Fig. 2.

It is striking to see on Fig. 4 that, for higher Da , the bistable kinetics leads to formation of droplets of one steady state detaching from the fingers and invading the other stable steady state. As pure density fingering has no preferred

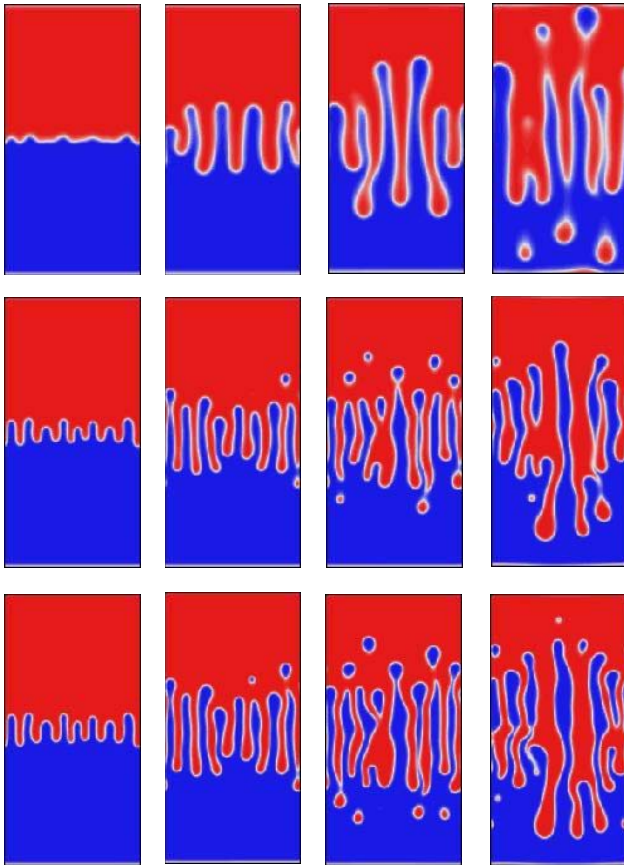


Fig. 4. Density fingering in the presence of chemical reactions. The Damköhler number is increased from top to bottom from $Da = 0.04, 0.14$ up to 0.20 , respectively, with $d = 0.5$ and $Pe = 512, A = 2$ as in Fig. 3. From left to right, the system is shown at successive times $t = 500, 1000, 1500$ and 2000 .

direction of propagation, it features the same extension of upwards and downwards fingers with respect to the initial position of the front when the density profile is linear (Wooding, 1969; Manickam & Homsy, 1995; Fernandez, Kurowski, Petitjeans, & Meiburg, 2002). Consequently, there will on average be as much droplets detaching from the bottom than from the top. The mechanism of formation of droplets is the same as that for viscous fingering with bistable kinetics (De Wit & Homsy, 1999a, b). In both cases, the high-mobility fluid enters the finger and encounters less mobile fluid at the tip of the fingers. This meeting obliges the turn away of the more mobile solution which is reentering the back of the finger as the fluid is incompressible. Hence, each finger is carrying a little vortex around its tip which leads to a decrease of the concentration behind the tip (see Fig. 4 for $Da = 0.04$ for instance). If the concentration at the location behind the tip crosses the value d of the unstable steady state, the concentration gets entrained by the other attractor and the system switches locally from one stable steady state to the other resulting in a pinching off of the tip. This tip then detaches from the bulk and gives rise to a droplet. The formation of droplets of one steady

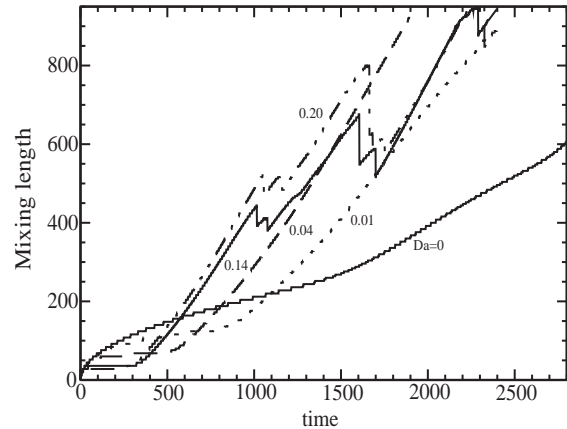


Fig. 5. Mixing length as a function of time for various values of the Damköhler number.

state into the other is thus a consequence of the bistable kinetics. The size of the droplets is immediately related to the size of the fingers at formation time. For $Da = 0.04$, the fingers are larger than for $Da = 0.14$ (see Fig. 4) and hence the droplets will on average be larger in the first case.

At the low Péclet value chosen here, no tip splitting is observed and density fingering alone leads to an overall coarsening of the fingers (Homsy, 1987). Hence, at later times far in the nonlinear regime, there are fewer and fewer fingers that become larger. The droplets formed will thus have increased size in the course of time. Such as in the case of viscous fingering, droplets are only transients. Ultimately, they all die as the critical radius above which one droplet of one steady state into the other steady state is growing in time is infinite for the bistable kinetics studied here (De Wit & Homsy, 1999a). We also remark that beyond a given value of Da , there is saturation of the influence of chemistry in the sense that there is not much difference in the wavelength and growth rate of the instability (compare $Da = 0.14$ and 0.20 in Fig. 4). The role of Da can further be analyzed looking at the mixing length of the fingers (see Fig. 5). This distance characterizing the mixing zone between the two solutions, is arbitrarily defined here as the zone for which $0.01 < \bar{c}(x, t) < 0.99$ where $\bar{c}(x, t)$ is the concentration profile averaged along the y direction. We note that the higher Da , the quicker the fingering characterized by a sudden linear increase of the mixing length after a certain transient. Abrupt decrease of the mixing zone corresponds to the death of droplets. Finally, let us note that, when $d \neq 0.5$, the planar reaction–diffusion front moves with a given velocity v . As has been shown for the case of viscous fingering, this does not affect the droplet formation scenario but leads to changes in the relative size of the droplets of both states as well as to entrainment of the fingers.

The dynamics resulting from the coupling between bistable chemical reactions with density fingering studied here shows similarities with the reactive viscous fingering studied by De Wit and Homsy (1999a, b). It is known that,

in absence of chemistry, the density-driven linear instability problem is equivalent to the viscous one when the density and viscosity profiles are both linear in c . For most fluids however, the density profile is linear as for IAA solutions for instance while the viscosity profile is nonlinear (as modeled by De Wit & Homsy, 1999a, b). In this case, connections exist also between the stability problems (Tan, 1987; Manickam & Homsy, 1995). The nonlinear dynamics on the other hand are not analogous since the coupling terms between the velocity and concentration fields are different for buoyancy and viscously driven cases (Rogerson & Meiburg, 1993; Manickam & Homsy, 1995). As an example, in density fingering, the extension of the mixing zone is symmetric with regard to the mean front position while it is not in viscous fingering because of the injection velocity. In presence of chemical reactions, these differences lead to a respectively symmetric and asymmetric averaged number of droplets with regard to the mean front position for density and viscous fingering. Besides this, the influence of the chemistry on the nonlinear dynamics looks quite analogous in both density and viscous-driven instabilities. The droplet formation mechanism is driven in each case by the rapid switch from one stable steady state to the other at the rear of the fingers. Reactive fingering leads also in both cases to fingers with smaller wavelengths appearing more quickly, i.e. the reactive system is more unstable. The balance between chemistry and hydrodynamics depends on the Damköhler number $Da = D\tau_c/U^2$ constructed with $U = \Delta\rho g\kappa/\nu$ for density fingering and with the injection velocity for viscous fingering. We observe that in both cases (a) droplet formation appears above a critical Da^l of order 0.01–0.02 on the time scale screened in our simulations; (b) there is another critical $Da^u \sim 0.12$ above which the effect of chemistry saturates; (c) the mixing lengths have analogous trends. Further studies are needed to have insight into the dynamics in presence of tip splittings for instance as well as more refined quantitative informations.

4. Spatial bistability in extended open reactors

The results of Sections 2 and 3 have been obtained making use of the CFUR approximation, i.e. considering a 2D reactor of area $l_x \cdot l_y$ assuming that the inflow and outflow along the orthogonal direction z are incorporated into the bistable kinetics as explained in the introduction. We now want to point out that the situation along the z axis is usually not trivial because of the existence of spatial bistability along z (Blanchedeau & Boissonade, 1998; Blanchedeau, Boissonade, & De Kepper, 2000; Borckmans et al., 2002).

To produce extended spatial systems leading to multiple steady states, the use of one-side fed reactors (OSFR) operated with reactions exhibiting HSS bistability in a CSTR is most appropriate. The usual advection-free OSFR reactors consist of a thin disk of gel (typically 0.2 mm thick) pressed against impermeable walls while one of its faces is in

contact with the contents of a CSTR (see Fig. 1b). Often an unidirectional porous inorganic membrane (e.g. Vycor from Corning Glass or Anotec from Whatman) is placed between both parts in order to rigidly maintain the disk of gel. In the context of the study of reaction–diffusion patterns the gel is a prerequisite in order to quench any perturbing hydrodynamical flow. The peculiar case of convective flows will be addressed later. So let us assume for the moment that we are still in a gel and that $\underline{u} = 0$.

The dynamics of an OSFR is described by the following set of equations, respectively, for the CSTR and the gel

$$\frac{\partial \mathbf{c}_s}{\partial t} = \mathbf{f}(\mathbf{c}_s) + \frac{(\mathbf{c}_s^0 - \mathbf{c}_s)}{\tau} + r_V \frac{D}{l_z} \left(\frac{\partial \mathbf{c}}{\partial z} \right)_{z=0}, \quad (16)$$

$$\frac{\partial \mathbf{c}}{\partial t} = \mathbf{f}(\mathbf{c}) + D\nabla^2 \mathbf{c}, \quad (17)$$

where \mathbf{c}_s^0 , \mathbf{c}_s and \mathbf{c} are the concentrations of the species, respectively, in the input flow of the CSTR, in the CSTR itself, and inside the gel, l_z is the thickness of the gel, r_V the ratio of the volume of the gel to the volume of the CSTR, and z the direction normal to the CSTR/gel interface. The \mathbf{f} 's are the reaction rates. In the right-hand side of Eq. (16), the second term represents the input and output flows of the species. It contains all the expandable control parameters of the system. The third term results from the diffusive flux of the species at the interface between the gel and the CSTR and represents the feedback of the gel contents on the CSTR dynamics. When the volume of the CSTR is large with regard to the volume of the gel ($r_V \ll 1$), this last term can usually be neglected so that the chemical state of the CSTR is independent of the state of the gel and the concentrations in the CSTR act as a Dirichlet boundary condition for Eq. (17) at $z = 0$ (in contact with the CSTR), whereas a no-flux boundary condition is applied at $z = l_z$ (along the impermeable wall). All other boundaries are impermeable.

Let us open a parenthesis to be more explicit about the IAA reaction. If all diffusion coefficients are equal, its kinetics may be reduced to the one variable kinetic function $f(c) = -qc(c - S_0)(c + \beta)$ as mentioned in Eq. (2) by making use of the conservation law of iodine species (iodide and iodate) which sum up to S_0 . The value of S_0 is imposed by the feeding of the CSTR whereas the relative values of iodide and iodate concentrations also result from the working conditions of the CSTR, i.e. essentially the residence time τ . We will consider that these conditions impose a concentration c_0 of iodide at the boundary between the CSTR and the gel. In the gel, the dynamics then reduces to the following one variable model written in dimensionless form:

$$\frac{\partial c}{\partial t} = -c(c - 1)(c + \gamma) + \frac{\partial^2 c}{\partial z^2}, \quad (18)$$

where $c = [I^-]/S_0$, $t = t^*/\tau$, $z = z^*/\sqrt{D\tau}$ with $\gamma = \beta/S_0 = k_a/k_b S_0 > 0$ and $\tau = 1/qS_0^2$. The dimensionless thickness of the gel is here $L_z = l_z/\sqrt{D\tau}$ with all starred quantities being dimensional. As stated before, because of the conservation law, the iodate concentration is simply $S_0(1 - c)$. The

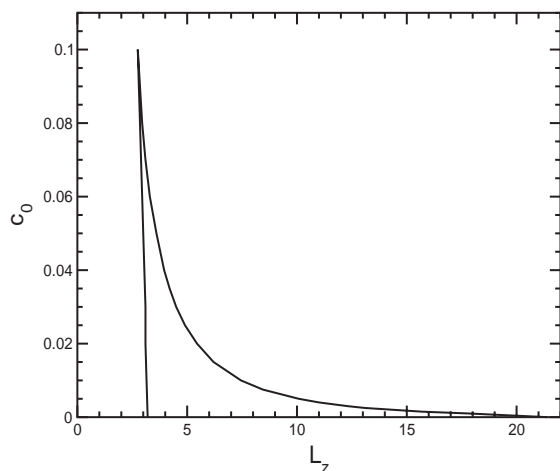


Fig. 6. Zone of spatial bistability in the $(c_0 - L_z)$ phase plane for $\gamma = 0.0021$. Below the curve, two different spatial profiles such as shown in Fig. 7 can coexist. If c_0 becomes too large, spatial bistability disappears. Outside the zone of spatial bistability, only one spatial solution is observed.

spatial term is written along the depth direction of the gel. Indeed, we do not expect spatial variations along the two other directions because the feeding is uniform and the diffusion coefficients are taken equal (no transverse patterning instabilities). The steady state concentration profiles are then given by

$$\frac{\partial^2 c}{\partial z^2} = c(c-1)(c+\gamma) \quad (19)$$

with the following boundary conditions: Dirichlet at the CSTR/gel interface:

$$c(z=0) = c_0 \quad (20)$$

and no flux at the impermeable wall and in particular

$$\left. \frac{\partial c}{\partial z} \right|_{z=L_z} = 0. \quad (21)$$

Owing to the presence of the CSTR, $0 < c_0 < 1$ as the 0 and 1 values would, respectively, correspond to zero or infinite residence time. Therefore no HSS may exist in the gel. The steady profiles can easily be obtained by a simple quadrature, however, they are in an implicit form and involve an elliptic function. Little insight can be gathered in such a procedure and one better resorts to numerical integration. Even for the simple IAA system considered here the result is by no means trivial and depends on the values of c_0 and L_z , the thickness of the gel slab, which are the sole parameters of the problem (Benyaich, Dewel, & Borckmans, 2003). Similar theoretical results have been obtained for reactions with more complex kinetics and have been corroborated experimentally (Blanchedeau & Boissonade, 1998; Blanchedeau et al., 2000). The main result is exhibited in the parameter space (c_0, L_z) (Fig. 6).

Inside the cusped region, Eq. (19) exhibits three inhomogeneous solutions satisfying the imposed boundary conditions. Two are stable while the remaining one is unstable

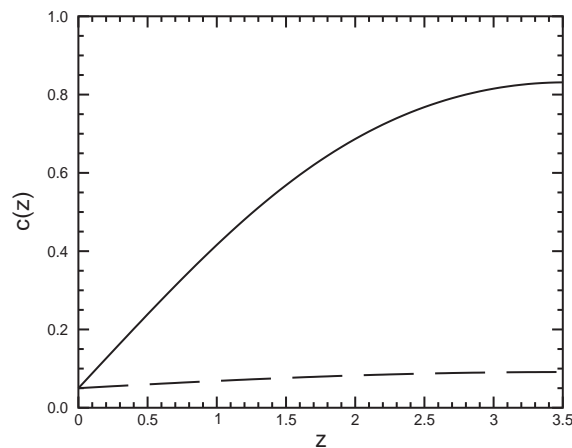


Fig. 7. Spatial bistability. Concentration along the gap width from $z = 0$ to L_z for $c_0 = 0.05$, $L_z = 3.5$ and $\gamma = 0.0021$. For the same values of parameters, the system can feature two different fronts represented here, respectively, in plain (up solution) and dashed (down solution) curves.

(we will not discuss metastability here). We see in Fig. 6 that state multiplicity only exists for rather small c_0 (weak iodide concentration in the CSTR). For a given c_0 , the bistability region of these profiles arises for intermediate thicknesses of the gel slab. An example of the profiles that may exist for completely identical conditions (hence the name *spatial bistability* attributed to the phenomenon) is shown in Fig. 7. One of the profiles (dashed line) varies only very weakly in space indicating that the concentration of iodide hardly changes in the z direction. The other profile corresponds to a switch where the iodide concentration steadily increases through the gel. The iodate profiles are complementary. Outside the cusped region of Fig. 6, only one profile exists and the system is monostable. For small L_z only the weakly varying profile remains, while for larger L_z only the switching state exists.

A typical bistability diagram exhibiting an hysteresis can be drawn plotting for instance the value of the iodide concentration $c(L_z)$ at the point furthest away from the CSTR/gel interface as a function of L_z (see Fig. 8). This diagram suggests that bistability between the profiles occurs through two back-to-back saddle–node bifurcations the loci of which trace the boundaries of the cusped region. The two profiles also differ by the iodide (and iodate) mass fluxes that cross the CSTR/gel interface. More detailed information on the phenomenon of spatial bistability may be found in Blanchedeau and Boissonade (1998); Blanchedeau et al. (2000) and Borckmans et al. (2002).

The results we have just discussed show that for a clock reaction such as the IAA, bistability arises from the competition between the chemical kinetics and mass fluxes that result from the feeding of the reactor. In the CSTR, bistability is between HSS because of the strong turbulent mixing while in the OSFR bistability is spatial and occurs

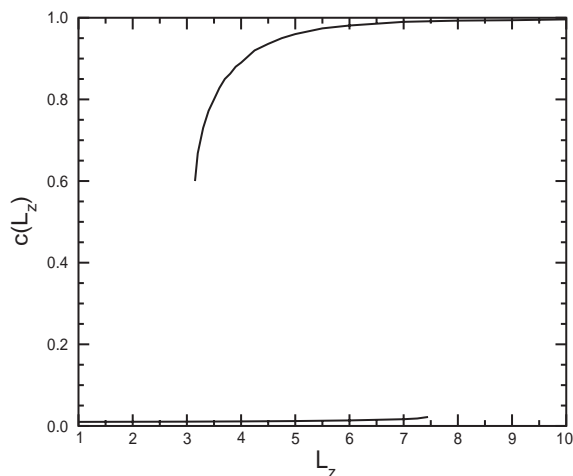


Fig. 8. Concentration at the edge $z = L_z$ of the system as a function of the gap width L_z . Here, $c_0 = 0.05$ and $\gamma = 0.0021$. There is a range of gap widths for which the system can feature both up and down solutions, a situation characterizing the spatial bistability.

between two concentration profiles maintained by the mass flux across the CSTR/gel boundary. In the conclusion, let us discuss how the concept of spatial bistability could be incorporated to experimentally visualize the density fingering and droplet detachment phenomena.

5. Conclusions

To produce experimentally spatially extended fronts between bistable states, we propose to use the principle of an OSFR where the gel would be replaced by a Hele–Shaw cell, one glass plate of which would be substituted by a sheet of a porous membrane in order to connect the cell to a CSTR (see Fig. 1). Convective phenomena are then again allowed inside the Hele–Shaw cell as in the experiments of Böckmann and Müller (2000), albeit they would be protected by the porous membrane from the turbulent flow in the CSTR. Such a device should allow the observation of the coupling between hydrodynamical motions and bistable kinetics. In particular, if the two chemical states have different densities, fingering phenomena as well as the droplet shedding could appear. However, the switching state along the z direction exhibits no steep front for the IAA system but a gradual change of concentration between a region of low iodide concentration close to the feeding boundary $z = 0$ to a high iodide concentration state deeper in the thickness of the gel ($z \rightarrow L_z$). Hence, the density of the medium varies accordingly along the z direction as the density is a decreasing function of iodide. This effect could be by itself the motor of convective motion in the gap even in the absence of a front connecting the two spatial bistable states along the xy plane as studied in Sections 2 and 3. Although this does not preclude the possibility of droplet formation this may render matter much more complicated.

Ideally, reactions with sharp jumps and reversible direction of propagation of the switch profile such as for the chlorine dioxide-iodide (CDI) reaction should be chosen (Blanchedeau et al., 2000). Furthermore, the unidirectional fine porous membranes (e.g. Vycor or Anotec membranes filled with a gel) of variable width could be used to absorb the steepest part of the gradient in the membrane part itself. One would thus be left in the rest of the reactor in conditions of uniformity close to the ideal ones used in Eqs. (4)–(7).

In conclusion, the use of a one-sided fed Hele–Shaw reactor could allow the experimental study not only of the fingering phenomena discussed here but also of many other pattern forming instabilities arising from the coupling between reaction, diffusion and convection in controlled open conditions.

Acknowledgements

We thank J. Boissonade and E. Dulos for fruitful discussions as well as the Van Buuren Foundation for financial support. A.D. acknowledges financial support from the FRFC (Belgium), Prodex (Contract 14556/00/NL/SFe(IC)) and ESA (Contract 15196/01/NL/SH). A.D., G.D. and P.B. are Research Associates at the FNRS (Belgium).

References

- Ackemann, T., Logvin, Yu. A., Heuer, A., & Lange, W. (1995). Transition between positive and negative hexagons in optical pattern formation. *Physical Review Letters*, *75*, 3450–3453.
- Bachir, M., Mérens, S., Borckmans, P., & Dewel, G. (2001). Formation of rhombic and superlattice patterns in bistable systems. *Europhysics Letters*, *54*, 612–618.
- Benyaich, K., Dewel, G., & Borckmans, P. (2003). Spatial bistability in simple reaction–diffusion models. Preprint.
- Blanchedeau, P., & Boissonade, J. (1998). Resolving an experimental paradox in open spatial reactors: The role of spatial bistability. *Physical Review Letters*, *81*, 5007–5010.
- Blanchedeau, P., Boissonade, J., & De Kepper, P. (2000). Theoretical and experimental studies of spatial bistability in the chlorine-dioxide-iodide reaction. *Physica D*, *147*, 283–299.
- Böckmann, M., & Müller, S. C. (2000). Growth rates of the buoyancy-driven instability of an autocatalytic reaction front in a narrow cell. *Physical Review Letters*, *85*, 2506–2509.
- Borckmans, P., Dewel, G., De Wit, A., Dulos, E., Boissonade, J., Gauffre, F., & De Kepper, P. (2002). Diffusive instabilities and chemical reactions. *International Journal of Bifurcation and Chaos*, *12*(11) 2307–2332.
- Breazeal, W., Flynn, K. M., & Gwinn, E. G. (1995). Static and dynamic two-dimensional patterns in self-extinguishing discharge avalanches. *Physical Review E*, *52*, 1503–1515.
- Carey, M. R., Morris, S. W., & Kolodner, P. (1996). Convective fingering of an autocatalytic reaction front. *Physical Review E*, *53*, 6012–6015.
- Chinake, C. R., & Simoyi, R. H. (1994). Fingering patterns and other interesting dynamics in the chemical waves generated by chlorite-thiourea reaction. *Journal of Physical Chemistry*, *98*, 4012–4019.
- Dewel, G., Mérens, S., Hilali, M. F., Borckmans, P., & Price, C. B. (1995). Resonant patterns through coupling with a zero mode. *Physical Review Letters*, *74*, 4647–4650.
- De Wit, A. (2001). Fingering of chemical fronts in porous media. *Physical Review Letters*, *87*, 054502.

- De Wit, A., & Homsy, G. M. (1999a). Viscous fingering in reaction–diffusion systems. *Journal of Chemical Physics*, *110*, 8663–8675.
- De Wit, A., & Homsy, G. M. (1999b). Nonlinear interactions of chemical reactions and viscous fingering in porous media. *Physics of Fluids*, *11*, 949–951.
- Edwards, B. F., Wilder, J. W., & Showalter, K. (1991). Onset of convection for autocatalytic reaction fronts in laterally unbounded system. *Physical Review A*, *43*, 749–760.
- Epstein, I. R., & Pojman, J. A. (1998). *An introduction to nonlinear chemical dynamics*. Oxford: Oxford University Press.
- Fernandez, J., Kurowski, P., Petitjeans, P., & Meiburg, E. (2002). Density-driven unstable flows of miscible fluids in a Hele–Shaw cell. *Journal of Fluid Mechanics*, *451*, 239–260.
- Firth, W. J., Scroggie, A. J., & McDonald, G. S. (1992). Hexagonal patterns in optical bistability. *Physical Review A*, *46*, R3609–R3612.
- Garbey, M., Taïk, A., & Volpert, V. A. (1998). Influence of natural convection on stability of reaction fronts in liquids. *Quarterly Applied Mathematics*, *56*, 1–35.
- Hanna, A., Saul, A., & Showalter, K. (1982). Detailed studies of propagating fronts in the iodate oxidation of arsenious acid. *Journal of American Chemical Society*, *104*, 3838–3844.
- Homsy, G. M. (1987). Viscous fingering in porous media. *Annual Reviews in Fluid Mechanics*, *19*, 271–311.
- Horváth, D., Bánsági, T. Jr., & Tóth, A. (2002). Orientation-dependent density fingering in an acidity front. *Journal of Chemical Physics*, *117*, 4399–4402.
- Huang, J., & Edwards, B. F. (1996). Pattern formation and evolution of autocatalytic reaction fronts in a narrow vertical slab. *Physical Review E*, *54*, 2620–2627.
- Lee, K. J., McCormick, W. D., Pearson, J. E., & Swinney, H. L. (1994). Experimental observation of self-replicating spots in a reaction–diffusion system. *Nature*, *369*, 215–218.
- Lee, K. J., & Swinney, H. L. (1995). Lamellar structures and self-replicating spots in a reaction–diffusion system. *Physical Review E*, *51*, 1899–1914.
- Manickam, O., & Homsy, G. M. (1995). Fingering instabilities in vertical miscible displacement flows in porous media. *Journal of Fluid Mechanics*, *288*, 75–102.
- Martin, J., Rakotomalala, N., Salin, D., & Böckmann, M. (2002). Buoyancy-driven instability of an autocatalytic reaction front in a Hele–Shaw cell. *Physical Review E*, *65*, 051605.
- Masere, J., Vasquez, D. A., Edwards, B. F., Wilder, J. W., & Showalter, K. (1994). Nonaxisymmetric and axisymmetric convection in propagating reaction–diffusion fronts. *Journal of Physical Chemistry*, *98*, 6505–6508.
- McCaughey, B., Pojman, J. A., Simmons, C., & Volpert, V. A. (1998). The effect of convection on a propagating front with a liquid product: Comparison of theory and experiments. *Chaos*, *8*, 520–529.
- Métens, S., Dewel, G., Borckmans, P., & Engelhardt, R. (1997). Pattern selection in bistable reaction–diffusion systems. *Europhysics Letters*, *37*, 109–114.
- Nagatsu, Y., & Ueda, T. (2001). Effects of reactant concentrations on reactive miscible viscous fingering. *AIChE Journal*, *47*, 1711–1720.
- Nagypal, I., Bazsa, G., & Epstein, I. R. (1986). Gravity-induced anisotropies in chemical waves. *Journal of American Chemical Society*, *108*, 3635–3640.
- Pearson, J. E. (1993). Complex patterns in a simple system. *Science*, *261*, 189–192.
- Pojman, J. A., Epstein, I. R., McManus, T. J., & Showalter, K. J. (1991). Convective effects on chemical waves. 2. Simple convection in the iodate arsenious acid system. *Journal of Physical Chemistry*, *95*, 1299–1306.
- Pojman, J. A., Gunn, G., Patterson, C., Owens, J., & Simmons, C. (1998). Frontal dispersion polymerization. *Journal of Physical Chemistry B*, *102*, 3927–3929.
- Rogerson, A., & Meiburg, E. (1993). Numerical simulation of miscible displacement processes in porous media flows under gravity. *Physics of Fluids A*, *5*, 2644–2660.
- Saul, A., & Showalter, K. (1985). In R. J. Field, & M. Burger (Eds.), *Oscillations and traveling waves in chemical systems*. New York: Wiley.
- Tan, C. T. (1987). *Stability of miscible displacements in porous media*. Ph.D. thesis, Stanford University, Stanford.
- Tan, C. T., & Homsy, G. M. (1988). Simulation of nonlinear viscous fingering in miscible displacement. *Physics of Fluids*, *31*, 1330–1338.
- Vasquez, D. A., Wilder, J. W., & Edwards, B. F. (1993). Hydrodynamic instability of chemical waves. *Journal of Chemical Physics*, *98*, 2138–2143.
- Vastano, J. A., Pearson, J. E., Horsthemke, W., & Swinney, H. L. (1987). Chemical pattern formation with equal diffusion coefficients. *Physical Letters A*, *124*, 320–324.
- Wooding, R. A. (1969). Growth of fingers at an unstable diffusing interface in a porous medium or Hele–Shaw cell. *Journal of Fluid Mechanics*, *39*, 477–495.
- Yang, J., D’Onofrio, A., Kalliadasis, S., & De Wit, A. (2002). Rayleigh–Taylor instability of reaction–diffusion acidity fronts. *Journal of Chemical Physics*, *117*, 9395–9408.